DETERMINING ELASTIC MODULI FOR PERCOLATION SYSTEMS

V. V. Novikov

A percolation model has been used to examine how the elastic moduli are affected by component bulk concentrations.

Formulation. Percolation theory deals with the structures and properties of microscopically inhomogeneous materials in which the components differ considerably in properties [1, 2]. The effective conductivity is derived in that theory (when $\sigma_1 \neq 0$, $\sigma_2 = 0$) as

$$\frac{\sigma}{\sigma_1} = \begin{cases} (v_1 - v_c)^t, & \text{if} \quad v_1 > v_c, \\ 0, & \text{if} \quad v_1 \leqslant v_c, \end{cases} \tag{1}$$

in which v_1 is the bulk concentration of the conducting component, v_c is the threshold, and t the critical index.

Simulation and measurements for three-dimensional systems show [2] that

$$v_c = 0{,}15 \pm 0{,}03, \; t = 1{,}5 - 2. \tag{2}$$

There have recently been discussions on the elastic parameters in percolation systems [3-10], where it has been found that the behavior of the conductivity and elasticity is very different from linearity in the bulk concentration. Calculations [5] show that when infinite clusters are formed (for $v_1 = v_c$), the system does not have macroscopic rigidity because near v_c the clusters are highly branched and contain many single links, and therefore on deformation they are compressed or stretched without elastic stress. In a face-centered cubic lattice, the threshold is [5] $v_c^* = 0.42$ (for $v_c = 0.119$), and the elastic moduli are

$$K \sim \mu \sim (v_1 - v_c^*)^f, \text{ where } f = 4.4 \pm 0.6. \tag{3}$$

A regular model has been proposed [6, 7], in which the angle between the units was fixed. In that model, macroscopic elasticity arises immediately the infinite cluster is formed. The critical index for a two-dimensional system was derived as $f = 3.3 \pm 0.5$.

These first studies indicated that v_c^* and f are dependent not only on the system dimensions but also on the component elasticities, as was found also in [9].

In [11, 12], percolation theory was used in a model (Fig. 1) that described the systems not only for $\sigma_2/\sigma_1 = 0$ but also for any finite values of that ratio in volume-concentration ranges from 0 to 1. In it, the isolated clusters (for $v_i < v_c$) are represented as cubes, with the links between those clusters arising suddenly for $v_i = v_c$ and being represented by square rods having areas of cross section

$$\bar{S}_1 = \left(\frac{v_1 - v_c}{1 - v_c}\right)^t. \tag{4}$$

For $v_1 < v_c$, the sizes of those clusters are proportional to $v_1^{1/3}$. Here there is an analogy with the droplet model [13], where a drop or blob is analogous to an isolated cluster.

Table 1 gives the geometrical parameters.

The Fig. 1 model has been used in [14] to derive formulas for K and μ in relation to the thermal-expansion coefficient for a two-phase system.

One can specify various t and v_c for the Fig. 1 model to examine the behavior of K and μ when the components differ considerably in properties: K μ.

Odessa Polytechnical Institute. Translated from Inzhenerno-Fizicheskii Zhurnal, Vol. 57, No. 3, pp. 485-490, September, 1989. Original article submitted February 18, 1988.

0022-0841/89/5703-1105$12.50 © 1990 Plenum Publishing Corporation

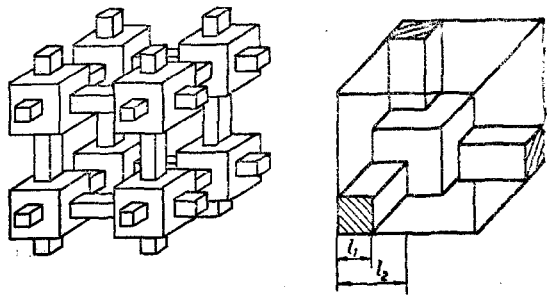

Fig. 1. Percolation model for a microscopically inhomogeneous material.

We consider how Poisson's ratio is dependent on the component concentrations and properties. The information may assist in interpreting simulation results and the behavior of K and μ.

Elastic Moduli. The elastic parameters are derived from the Fig. 1 model by means of two-sided bounds for the bulk modulus K [15]:

$$\{K(x_i,\ x_j)\}_S \leqslant K \leqslant [\{[K(x_k)]^{-1}\}_L]^{-1}, \tag{5}$$

and for the shear modulus

$$\{\mu(x_i,\ x_j)\}_S \leqslant \mu \leqslant [\{[\mu(x_k)]^{-1}\}_L]^{-1}, \tag{6}$$

in which

$$K(x_k) = \frac{\{KP\}_S}{\{P\}_S};\ \mu(x_k) = \{\mu\}_S, \tag{7}$$

$$K(x_i,\ x_j) = \left(\left\{\frac{n}{K}\right\}_L - 2\frac{\{d\}_L\{P\}_L}{\{KP\}_L}\right)^{-1},\ \mu(x_i,\ x_j) = \{\mu^{-1}\}_L^{-1}. \tag{8}$$

Here the braces represent averaging over the coordinates:

$$\{f(\mathbf{r})\}_L = \frac{1}{L}\int_0^L f(\mathbf{r})\,dx_k,\ \{f(\mathbf{r})\}_S = \frac{1}{S}\iint_{(S)} f(\mathbf{r})\,dx_i dx_j, \tag{9}$$

in which L is the length of the representative volume V along the Ox_k axis, while S is the cross section of V in the plane x_k = const.

The (5) and (6) bounds can be used with stage averaging when the entire representative volume V is split up into parts, from which the effective parameters are determined and then the formulas are used for the upper and lower bounds (combined method). That procedure gives formulas for the effective properties, which can be used in calculations on the values within the possible ranges and the related arithmetic means.

From (4) and (5) with stage averaging [15] we determined the effective elastic moduli K and μ, for which formulas are given in the Appendix.

Results. Figure 2 shows calculations on the effective Poisson's ratio ν. Curves 1, 3, and 5 are for $t = 1.6$ $v_c = 0.15$ while 2, 4, and 6 are for $t = 3.6$, $v_c = 0.3$. Curves 1-4 are for $K_2/K_1 = 10^{-4}$, with $\mu_1/K_1 = 0.3$, $\mu_2/K_2 = 10^{-2}$, for curves 1 and 2, and $\mu_1/K_1 = 0.255$; for curves 3 and 4. Curves 5 and 6 are for $K_2/K_1 = 6.75\cdot10^{-3}$, $\mu_1/K_1 = 0.773$, $\mu_2/K_2 = 0.255$. Figure 2 implies that ν is substantially dependent not only on v_c and t but also on μ_1/K_1 and μ_2/K_2, where curves 3 and 4 are of interest, as there is a nonmonotone dependence of ν on concentration: curve 3 has a minimum around the transition from an infinite cluster to an isolated form of cluster for the rigid component, while curve 4 has two turning points near the transition from isolated clusters to an infinite one (minimum) and the converse (maximum) for the rigid component. Curves 1 and 2 ($\mu_1/K_1 = 0.3$, $\mu_2/K_2 \cong 0$) are convex upwards, while 3 and 5 are convex downwards, i.e., the concentration dependence of ν varies substantially with changes in μ_1/K_1 and μ_2/K_2.

TABLE 1. Percolation-Model Geometrical Parameters*

v_1 range	$S_1^{(M)}$	S_2	S_3	S_4	l_1	l_2
$0 \leqslant v_1 \leqslant v_c$	0	$v_1^{2/3}$	0	$1-v_1^{2/3}$	0	$v_1^{1/3}$
$v_c < v_1 \leqslant 0{,}5$	$\frac{1}{3}\frac{v_1-v_c}{1-v_c^{1/3}}$	$v_c^{2/3}-S_1^{(M)}$	$2l_1(1-l_2)$	$1-l_2^2-S_3$	$S_1^{1/2}$	$v_c^{1/3}$

*) $S_1=\overline{S}+(S_1^{(M)}-\overline{S})\,g(z)$, $\overline{S}=\left(\frac{v_1-v_c}{1-v_c}\right)^t$, $g(z)=5{,}53z-8{,}3z^2+3{,}23z^3+0{,}54z^4$, $z=K_2/K_1$, $K_2<K_1$.

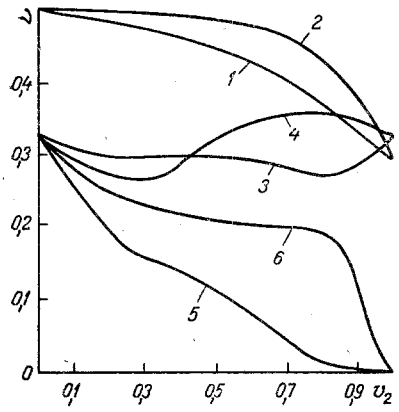

Fig. 2

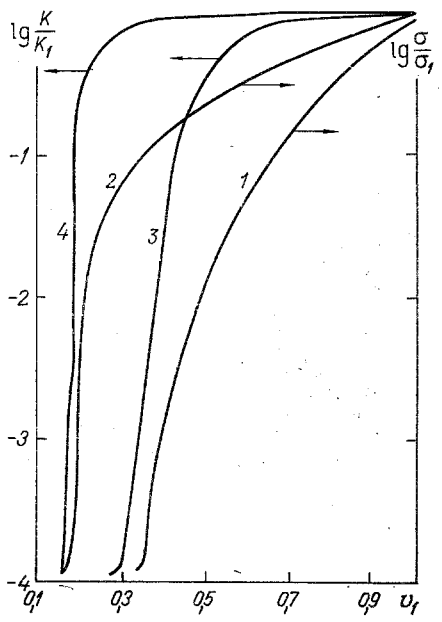

Fig. 3

Fig. 2. Poisson's ratio as a function of the bulk concentration v_2 of the soft component, the curves being by calculation for 1, 2) $K_2/K_1 = 10^{-4}$, $\mu_1/K_1 = 0.3$, $\mu_2/K_2 \cong 10^{-2}$ (1 – t = 1.6, v_c = 0.15; 2) t = 3.6, v_c = 0.3); 3, 4) $K_2/K_1 = 10^{-4}$ $\mu_1/K_1 = \mu_2/K_2$ = 0.255 (3 – t = 1.6, v_c = 0.15; 4) t = 3.6 v_c = 0.3); 5, 6) K_2/K_1 = $6.75\cdot10^{-3}$, $\mu_2/\mu_1 = 2.1155\cdot10^{-3}$, μ_1/K_1 = 0.773, μ_2/K_2 = 0.255 (5 – t = 1.6, v_c = 0.15; 4 – t = 3.6, v_c = 0.3).

Fig. 3. K/K_1 and c/c_1 as functions of v_1, the bulk concentration of the rigid component: 1, 2) $\sigma_2/\sigma_1 = 10^{-4}$ (1 – t = 1.6, v_c = 0.15; 2 – t = 3.6, v_c = 0.3); 3, 4) $K_2/K_1 = 10^{-4}$, $\mu_1/K_1 = \mu_2/K_2$ = 0.255, (3 – t = 1.6, v_c = 0.15; 4 – t = 3.6, v_c = 0.3).

Figure 3 shows calculations on K and σ. There are differences in behavior for the same v_c and t: a sharper increase in log K/K_1 near the threshold ($v_1 \sim v_c$) by comparison with that in log σ/σ_1 and a weak dependence of log K/K_1 on v_1 for $v_1 \gg v_c$, i.e., $\frac{\partial(\lg K/K_1)}{dv_1} < \frac{\partial(\lg\sigma/\sigma_1)}{\partial v_1}$, for $v_1 > v_c$. If $\mu_1/K_1 = \mu_2/K_2$, the v_1 dependence of $\lg K/K_1$ is close to that for $\lg\sigma/\sigma_1$.

If K is represented as in (5), f and v_c^* are dependent on μ_1/K_1 and μ_2/K_2, i.e., v_c^* and f are not universal parameters for the elastic parameters, in contrast to the conductivity. Therefore, additional measurements are required to refine v_c^* and f.

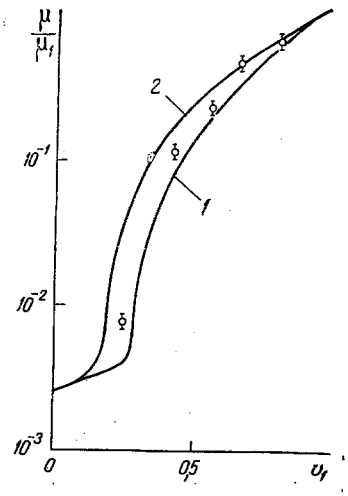

Fig. 4. Dependence of μ/μ_1 on the polystyrene bulk concentration v_1, curves from calculation: 1) v_c = 0.2, t = 1.6; 2) v_c = 0.15, t = 1.6, points from experiment [16].

The threshold should be defined as $v_c = 0.15 \pm 0.03$ in calculating the elastic parameters for microscopically inhomogeneous materials from the Fig. 1 model because in that model v_c is a topological characteristic, not the value for the bulk concentration at which rigidity arises. Here f is taken as 1.6-2 because in that model it is not dependent on the component properties, while the Poisson's ratios ν_i for the components affect K and μ in this model in a way that is incorporated directly in specifying the input data.

Materials showing percolation effects for the elastic properties are composites of polymer-polymer type.

Figure 4 compares calculations from (11) with measurements on μ/μ_1 for a polybutadiene-polystyrene composite, which gives quite good agreement. An infinite cluster is formed here when $0.15 < v_1 <_1 < 0.2$, i.e., $v_c = 0.175 \pm 0.025$, and the critical index is t = 1.6.

APPENDIX

The bulk modulus is

$$K = \frac{\varkappa_3 h_3 (S_2 + S_3) + \varkappa_4 h_4 (S_1 + S_4)}{h_3 (S_2 + S_3) + h_4 (S_1 + S_4)}, \tag{10}$$

in which

$$\varkappa_4 = \frac{K_1 P_1 S_1 + K_2 P_2 S_2}{P_1 S_1 + P_2 S_2};$$

$$\varkappa_3 = \frac{\varkappa_1 h_1 S_2 + \varkappa_2 h_2 S_3}{h_1 S_2 + h_2 S_3};$$

$$\varkappa_2 = \left\{ \frac{n_1}{K_1} l_1 + \frac{n_2}{K_2} (1 - l_1) - 2 \frac{[d_1 l_1 + d_2 (1 - l_1)]\,[P_1 l_1 + P_2 (1 - l_1)]}{K_1 P_1 l_1 + K_2 P_2 (1 - l_1)} \right\}^{-1};$$

$$\varkappa_1 = \left\{ \frac{n_1}{K_1} l_2 + \frac{n_2}{K_2} (1 - l_2) - 2 \frac{[d_1 l_2 + d_2 (1 - l_2)]\,[P_1 l_2 + P_2 (1 - l_2)]}{K_1 P_1 l_2 + K_2 P_2 (1 - l_2)} \right\}^{-1};$$

$$n_i = \frac{9}{(3 + 4m_i)}; \quad P_i = \frac{6m_i}{3 + 4m_i};$$

$$d_i = \frac{3 - 2m_i}{3 + 4m_i}; \quad m_i = \mu_i / K_i, \quad i = 1, 2.$$

The shear modulus is

$$\mu = \gamma_3 (S_2 + S_3) + \gamma_4 (S_1 + S_4), \tag{11}$$

in which

$$\gamma_4 = \mu_1 \frac{S_1}{S_1 + S_4} + \mu_2 \frac{S_4}{S_1 + S_4};$$

$$\gamma_3 = \gamma_1 \frac{S_2}{S_2 + S_3} + \gamma_2 \frac{S_3}{S_2 + S_3};$$

$$\gamma_2 = \left(\frac{l_1}{\mu_1} + \frac{1 - l_1}{\mu_2} \right)^{-1}, \quad \gamma_1 = \left(\frac{l_2}{\mu_1} + \frac{1 - l_2}{\mu_2} \right)^{-1}.$$

If the combined concentration is $v_1 > 0.5$, the subscripts 1 and 2 are interchanged in K_i and μ_i in (10) and (11) and for v_i in Table 1.

LITERATURE CITED

1. S. Kirkpatrick, Rev. Mod. Phys., 45, 473-485 (1973).
2. V. I. Shklovskii and A. L. Efros, Doped-Semiconductor Electronic Parameters [in Russian], Moscow (1979).
3. D. J. Bergman, Phys. Rev. B, 31, 1696-1698 (1985).
4. D. Deptuck, J. P. Harrison, and P. Zawadzki, Phys. Rev. Lett., 54, 913-916 (1985).
5. S. Feng and P. N. Sen, Phys. Rev. Lett., 52, 216-219 (1984).
6. Y. Kantor and J. Webman, Phys. Rev. Lett., 52, 1892-1897 (1984).
7. S. Feng, P. N. Sen, B. J. Halperin, and C. Lobb, Phys. Rev., B9, 5386-5394 (1984).
8. L. Benquigui, Phys. Rev. Lett., 53, No. 21, 2028-2030 (1984).
9. M. I. Gai, L. I. Manevich, and V. G. Oshmyan, Dokl. Akad. Nauk SSSR, 276, No. 6, 1389-1391 (1984).
10. M. I. Gai, E. S. Zelinskii, L. I. Manevich, et al., The Mechanics of Composite Materials [in Russian], No. 2 (1987), pp. 243-249.
11. G. N. Dul'nev and V. V. Novikov, Inzh. Fiz. Zh., 36, No. 5, 900-909 1979).
12. G. N. Dul'nev and V. V. Novikov, Inzh. Fiz. Zh., 45, No. 3, 443-451 (1983).
13. A. P. Vinogradov and A. K. Sarychev, Zh. Éksp. Teor. Fiz., 85, 1144 (1983).
14. V. V. Novikov, Inzh. Fiz. Zh., 47, No. 4, 617-624 (1984).
15. V. V. Novikov, Zh. Prikl. Mat. Tekh. Fiz., No. 5, 146-153 (1985).
16. W. Y. Hsu, M. R. Giri, and R. H. Ikeda, J. Am. Chem. Soc., 15, No. 4, 1210-1213 (1982).

RADIAL ELECTRON DENSITY DISTRIBUTION IN PLASMA FLOW IN A COAXIAL HALL ACCELERATOR

I. A. Anoshko, V. S. Ermachenko, M. N. Rolin, V. G. Sevast'yanenko, and L. E. Sandrigailo

UDC 533.9.082

The values of the electron density determined from measurements of the Starr broadening of a hydrogen line are presented.

Plasma accelerators are employed in diverse areas of science and technology. To increase their operating efficiency it is necessary to study the physical processes occurring in the plasma jet. Information about these processes can be obtained from measurements of the temperature and particle density.

In this paper we present the results of measurements of the electron density in the plasma flow in a coaxial Hall accelerator; the principle of operation and the construction of the accelerator are described in [1, 2]. The electron density was determined in the section of the plasma jet located 130 mm from the cutoff of the nozzle of the accelerator; the flow rate of the working gas C_Σ = 10 g/sec (8.5 g of air and 1.5 g of nitrogen), the magnetic

A. V. Lykov Institute of Heat and Mass Transfer, Academy of Sciences of the Belorussian SSR. Belorussian Polytechnical Institute, Minsk.

Translated from Inzhenerno-Fizicheskii Zhurnal, Vol. 57, No. 3, pp. 491-493, September, 1989. Original article submitted February 24, 1988.